Effect of Polyurethane Viscosity on Self-Healing Efficiency of Cementitious Materials Exposed to High Temperatures from Sun Radiation

B. Van Belleghem[1]; E. Gruyaert[2]; K. Van Tittelboom[3]; W. Moerman[4]; B. Dekeyser[5]; J. Van Stappen[6]; V. Cnudde[7]; and N. De Belie[8]

Abstract: Insulated concrete elements used in building facades, e.g., sandwich panels, are frequently exposed to sun radiation, which causes high temperatures on the outside. Although the inner and outer cladding are supposed to be independent, a high temperature difference between the outside and the inside of the elements causes thermal bending, which can lead to cracking. These cracks may have an impact on the durability of the outer cladding and are not wanted from an esthetic point of view. A possible solution for this problem is the embedment of encapsulated polyurethane in the concrete matrix in order to repair cracks autonomously. However, healing agents with suitable properties are needed to heal cracks at these conditions. In this research, newly developed polyurethane resins with relatively high viscosity were tested for their healing efficiency at high temperatures. The mechanical properties of the polyurethanes such as bond strength and elasticity were determined. Second, the healing agents were encapsulated and evaluated for their efficiency to heal cracks by capillary absorption tests, strength regain evaluation, and X-ray computed tomography. The new polyurethanes were much more elastic than the commercially available ones and thus more able to withstand opening and closing of cracks due to temperature changes. The water ingress in specimens with healed cracks was found to decrease with increasing viscosity of the polyurethanes. At a temperature of 50°C, the polyurethanes were able to heal cracks so that the water absorption of cracked mortar was reduced to a value that was comparable to the water absorption of uncracked mortar. Also, a strength regain of 100% or more was obtained. Therefore, using self-healing concrete in building facades may have a positive effect on the durability and service life of the construction elements. **DOI: 10.1061/(ASCE)MT.1943-5533.0002360.** © *2018 American Society of Civil Engineers.*

[1]Ph.D. Candidate, Magnel Laboratory for Concrete Research, Dept. of Structural Engineering, Faculty of Engineering and Architecture, Ghent Univ., Technologiepark Zwijnaarde 904, B-9052 Ghent, Belgium; Strategic Initiative Materials, Technologiepark Zwijnaarde 935, B-9052 Ghent, Belgium (corresponding author). Email: bjorn.vanbelleghem@UGent.be

[2]Professor, Dept. of Civil Engineering, Technology Cluster Construction, Structural Mechanics and Building Materials, KU Leuven, Gebroeders De Smetstraat 1, B-9000 Ghent, Belgium.

[3]Professor, Magnel Laboratory for Concrete Research, Dept. of Structural Engineering, Faculty of Engineering and Architecture, Ghent Univ., Technologiepark Zwijnaarde 904, B-9052 Ghent, Belgium; Strategic Initiative Materials, Technologiepark Zwijnaarde 935, B-9052 Ghent, Belgium.

[4]Professor, Magnel Laboratory for Concrete Research, Dept. of Structural Engineering, Faculty of Engineering and Architecture, Ghent Univ., Technologiepark Zwijnaarde 904, B-9052 Ghent, Belgium; Willy Naessens Construct, Bedrijvenpark Coupure 15-17, B-9700 Oudenaarde, Belgium.

[5]R&D Engineer, R&D Dept., Recticel N.V., Damstraat 2, B-9230 Wetteren, Belgium.

[6]Ph.D. Candidate, PProGRess–UGCT, Dept. of Geology, Faculty of Sciences, Ghent Univ., Krijgslaan 281 S8, B-9000 Ghent, Belgium.

[7]Professor, PProGRess–UGCT, Dept. of Geology, Faculty of Sciences, Ghent Univ., Krijgslaan 281 S8, B-9000 Ghent, Belgium.

[8]Professor, Magnel Laboratory for Concrete Research, Dept. of Structural Engineering, Faculty of Engineering and Architecture, Ghent Univ., Technologiepark Zwijnaarde 904, B-9052 Ghent, Belgium.

Note. This manuscript was submitted on August 28, 2017; approved on January 30, 2018; published online on May 11, 2018. Discussion period open until October 11, 2018; separate discussions must be submitted for individual papers. This paper is part of the ***Journal of Materials in Civil Engineering***, © ASCE, ISSN 0899-1561.

Introduction

Concrete is one of the most widely used construction materials. Although it has a lot of good properties, it is also very vulnerable to crack formation. Steel reinforcement is used in concrete to limit the crack width, but it cannot completely prevent crack formation. A common example is thermal cracking of insulated concrete elements used in building facades. During the last few decades, a lot of attention has been given to energy efficiency in the building industry. Nowadays, every building has to meet certain criteria regarding energy efficiency and thermal insulation capacity. For this reason, the building industry has started to move toward the use of insulated concrete sandwich panels for buildings. Next to the advantages regarding energy consumption, the insulation layer is both lightweight and contributes to reducing the building's energy consumption.

Concrete sandwich panels consist of an outer concrete cladding; an insulation layer consisting mostly of rigid foam materials like polyurethane, polystyrene, or phenolic foam (Ahmad and Mohammad 2012); and an inner concrete cladding. When there is sun radiation at the outer cladding of the element, the presence of the insulation layer causes a high temperature difference between the outside and the inside of the element. This high temperature difference may cause thermal bending (Salmon and Einea 1995), which can lead to crack formation in the outer concrete cladding. These cracks can impair the durability of the outer cladding since aggressive agents can enter the concrete matrix through the cracks and cause deterioration. Moreover, the cracks are also unwanted from an esthetic point of view.

During the past 20 years, the embedment of self-healing properties in the concrete matrix in order to repair cracks autonomously

has become a growing research topic (Li et al. 1998; Dry et al. 2003; Mihashi and Nishiwaki 2012). One of the promising possibilities is autonomous crack healing by means of encapsulated healing agents (Van Tittelboom et al. 2011b; Feiteira et al. 2016). Upon crack appearance, the capsules break and release the healing agent, causing crack repair. In order to use this self-healing principle for crack repair of thermal bending cracks, the choice of healing agent is very important. Different healing agents have already been tested for their efficiency in self-healing concrete, for example, cyanoacrylate (Dry 2001), epoxy (Dry 2001), methyl methacrylate (Dry and McMillan 1996; Van Tittelboom et al. 2011a), and polyurethane (Van Tittelboom et al. 2011b; Maes et al. 2014). Among them, polyurethane is the healing agent with the most promising properties for the current application. It has a low molecular weight and small molecular size, which allows it to permeate into small pores and narrow cracks. It is also very flexible and available in a wide range of viscosities (Petrie 2007).

Most of the research works on self-healing concrete are done at a temperature of 20°C. However, in case cracking occurs due to thermal actions by sun radiation, it is necessary to choose healing agents with suitable properties at high temperatures in order to obtain a satisfactory healing efficiency.

In previous research (Van Tittelboom et al. 2015), polyurethane has been used for self-repair of thermal cracks in concrete sandwich panels. For the two types of polyurethane precursors used in that research, a lot of leaching was noticed at the surface when the healing action was triggered. Therefore, it was concluded that the viscosity of the healing agent should be increased. The healing agent should have a suitable viscosity at a temperature of around 50°C since the surface temperature of a concrete element can be up to 52°C when the outside temperature is 35°C on a summer day (Van Belleghem 2014). Another important conclusion from the research of Van Tittelboom et al. (2015) was that the polyurethane was detached from the surface at some locations. As thermal cracks in sandwich panels open and close, the healing agent needs to be flexible enough after release and repair to be able to follow the movement of cracks due to temperature cycles.

The main focus of this research was the investigation of the impact of the viscosity of the healing agent on the self-healing potential of concrete exposed to high temperatures. Therefore, some properties of the polyurethanes regarding elasticity were investigated by axial tensile tests. Subsequently, the polyurethanes were encapsulated and their healing efficiency at low (20°C) and high (50°C) temperatures was compared by water absorption tests. Afterward, the strength regain due to crack healing was studied by reloading the specimens. For some of the specimens, X-ray computed tomography (XCT) (Cnudde and Boone 2013) was used as a nondestructive method to evaluate crack healing (Van Tittelboom et al. 2010, 2011b, 2016; Wang et al. 2014).

Materials

Healing Agents

Five one-component polyurethane precursors were developed in this research. The different products were denoted by the codes A to E. The precursors had a similar chemical composition, but descending viscosities and ascending isocyanate (NCO) contents. The viscosities of the precursors were measured at 20 and 50°C and are given in Table 1 together with the NCO content. The exact composition of the precursors should remain confidential. The use of one-component polyurethane precursors was preferred to multicomponent healing agents because of the risk of incomplete mixing of the different components after being released in the crack. Moreover, the used products have a volume increase by a foaming reaction upon contact with moisture. In this way it is possible to fill larger crack volumes.

Table 1. Viscosity and NCO content of the newly developed polyurethane precursors

Specimen	Viscosity at 20°C (mPa · s)	Viscosity at 50°C (mPa · s)	NCO (%)
A	17375	1835	4.8
B	12028	1515	5.8
C	8040	1154	7.1
D	6150	941	8.2
E	4120	675	9.8

Next to the newly developed polyurethanes, two commercially available polyurethanes were used in order to compare their efficiency. The commercial polyurethane precursors are one-component polyurethanes that have been tested in the past at Ghent University for their efficiency in self-healing concrete (Feiteira et al. 2014, 2016). The products will be referred to as LV and SLV, denoting low viscosity and super low viscosity. The viscosities of the precursors at 25°C are 550 and 200 mPa · s, respectively.

Glass Capsules

For proof of concept, encapsulation of the healing agents was done by using cylindrical borosilicate glass capsules with a length of 50 mm, an internal diameter of 3 mm, and an outer diameter of 3.35 mm. Because glass is a very brittle material, the capsules will easily break when cracks appear in the cementitious matrix. Also, glass has excellent barrier properties, preventing a reaction of the precursor inside the capsules with the moist concrete surrounding.

The glass capsules were sealed with polymethyl methacrylate (PMMA) at one end. Subsequently, the healing agents were carefully injected into the glass capsules by means of a syringe with a needle. Finally, the other ends of the capsules were also sealed with PMMA.

Cylindrical Mortar Specimens

In order to determine the bond strength and elasticity of the different polyurethanes, axial tensile tests were performed (Feiteira et al. 2016). For these tests, the precursors were applied between two mortar cylinders. A standard mortar mix with a water to cement ratio of 0.4 and a sand to cement ratio of 3 was made according to the European standard EN 196-1 (European Committee for Standardization 2016). Ordinary portland cement (CEM I 52.5 N) was used in combination with sand with grain size 0–2 mm. Mortar prisms with dimensions of $150 \times 150 \times 600$ mm were cast and stored at 20 ± 2°C and 95% relative humidity for 28 days. After the curing period, cylinders with a diameter of 50 mm and a height of 150 mm were drilled out of the prisms. The drilled cylinders were then cut in half to obtain a pair of cylinders, each with a height of around 70 mm. These pairs of cylinders were then stored at a temperature of 20 ± 2°C and a relative humidity of 60% until constant mass was achieved (mass change less than 0.1% in 24 h).

Prismatic Mortar Specimens

To determine the healing efficiency of the different polyurethanes, prismatic mortar specimens were prepared using a standard mortar mix as described in the previous section, but with a water to cement

Fig. 1. (a) Molds used for creation of prismatic mortar specimens with dimensions of $40 \times 40 \times 160$ mm with two reinforcement bars (diameter = 3 mm); and (b) three capsules filled with a polyurethane precursor are fixed on nylon threads between the reinforcement bars.

ratio of 0.5. The specimens had dimensions of $40 \times 40 \times 160$ mm and were cast in wood formworks. The mortar samples were reinforced by means of two steel bars containing screw thread with a diameter of 3 mm. The reinforcement bars were positioned at 10 mm from the bottom and at 10 mm from the sides of the prisms. In this way, the spacing between the bars was 20 mm. All specimens, except the reference samples, also contained three capsules filled with one of the newly developed polyurethane precursors. The position of the capsules was fixed by gluing them on thin nylon threads between the reinforcement bars in the middle of the prisms (Fig. 1). After the placement of the capsules, a first mortar layer of 20 mm was put in the molds and compacted by means of vibration. Subsequently, the molds were completely filled and vibrated again. The surface of the specimens that was not in contact with the formwork was flattened manually after compaction. For each of the five developed polyurethane precursors, six prismatic mortar samples were prepared. After casting, all specimens were placed in an air-conditioned room with a temperature of 20 ± 2°C and a relative humidity of at least 95%. The prisms were demolded after 24 h and stored under the same conditions for 14 subsequent days. After this period, three mortar samples of each series (each type of precursor) were stored in a climatized room at 20 ± 2°C and the other three samples were stored in an oven at 50 ± 2°C for a period of 14 days. The temperature of 50°C was chosen because of the fact that the outer surface of a concrete element can reach temperatures up to 52°C on a hot summer day, as mentioned previously. However, in a realistic environment it is impossible for a concrete element to continuously experience a temperature of 50°C for 14 days. During a hot period, the temperature will vary between 20 and 50°C.

An overview of the different prismatic mortar specimen series is given in Table 2. Each series contained three replicate specimens.

Table 2. Overview of the prismatic mortar specimen test series

Specimen	Description of test series	Storage temperature (°C)
UNCR	Uncracked mortar specimens	20
CR	Cracked mortar specimens	20
A (20°C)	Cracked mortar specimens	20
A (50°C)	healed with Product A	50
B (20°C)	Cracked mortar specimens	20
B (50°C)	healed with Product B	50
C (20°C)	Cracked mortar specimens	20
C (50°C)	healed with Product C	50
D (20°C)	Cracked mortar specimens	20
D (50°C)	healed with Product D	50
E (20°C)	Cracked mortar specimens	20
E (50°C)	healed with Product E	50

Methods

Crack Formation

At the age of 21 days, a crack was created in the prismatic mortar specimens by means of a three-point bending test (except for the uncracked reference series). For the specimens containing capsules, the creation of the crack caused the capsules to break and release the healing agent in the crack. The crack width was continuously measured during the bending test by means of an LVDT with a measurement range of 1 mm. The LVDT was attached to the specimen by a small metal block that was glued to the bottom of the sample. The crack width was increased with a velocity of 3 μm/s until a crack width of 700 μm was obtained. Then the specimens were unloaded causing a decrease in crack width. The final crack width was between 150 and 300 μm. A detailed description and schematic figure of the three-point bending test setup can be found in Van Tittelboom et al. (2011b).

All of the mortar samples, the ones stored at 20°C and the ones stored at 50°C, were taken out of their environment, loaded by a three-point bending test, and placed back in their respective environments immediately after loading. In this way the hardening of the polyurethane inside the cracks took place at the respective storage temperatures.

Determination of Bond Strength and Elasticity of the Polyurethanes

The healing efficiency and the ability of a healing agent to follow crack movements depends on the elasticity of the healing agent, the strength of the healing agent, and the bond strength between the mortar–concrete matrix and the healing agent. Axial tensile tests on the different polyurethanes were performed to determine these properties. As mentioned previously, mortar cylinders were used for these tests. An artificial crack of 300 μm was obtained by placing a pair of mortar cylinders on top of each other with spacers (thickness of 300 μm) in between. First, the spacers were put on one mortar cylinder, then 0.6 mL of precursor was applied in the middle of the surface of the cylinder, and finally the second mortar cylinder was put on top of the first one. The volume of the precursor that was applied (0.6 mL) corresponds more or less to the theoretically calculated volume of the simulated crack (589 mm^3). Three pieces of paper tape were then placed over the crack on the sides of the mortar cylinders. In this way the simulated crack was not exposed to the air along the whole circumference, so a more realistic crack environment was obtained. The final samples were stored for 14 days in an air-conditioned room with a temperature of 20 ± 2°C and a relative humidity of 60%. For each of the polyurethanes, three replicate samples were tested.

After 14 days, the paper tape was removed from the samples and they were subjected to an axial tensile test. In order to fix the samples in the testing machine, metal dollies were glued to the end faces of the samples with a two-component epoxy glue. During the test, the applied force was measured by a load cell and the elongation of the polyurethane was measured by three LVDTs. The LVDTs were fixed along the circumference of the sample by plastic

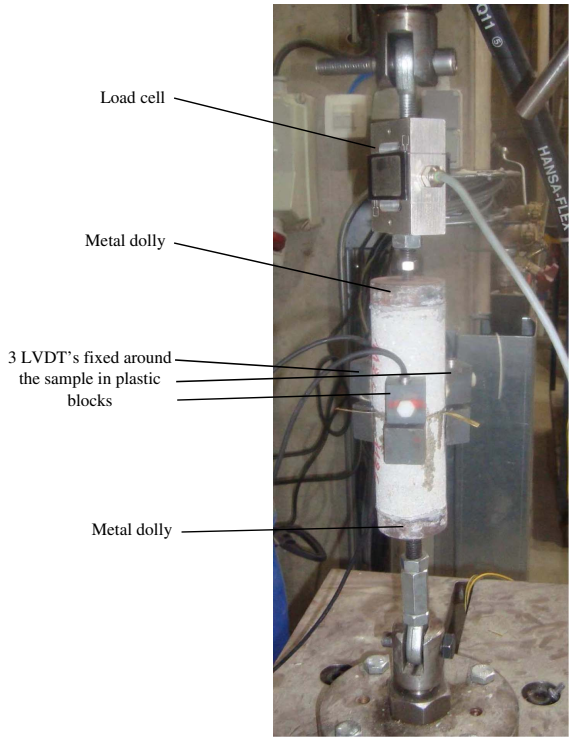

Fig. 2. Sample with a simulated crack of 300 μm filled with polyurethane fixed in the testing machine before the performance of a displacement-controlled axial tensile test.

blocks that were glued onto the sample. After the sample was fixed into the testing machine (Fig. 2), a displacement-controlled tensile test was performed with a velocity of 1 mm/min. From the resulting loading curve, the maximum load and the elongation at failure of the different polyurethanes could be determined.

After the tensile tests, the fracture surfaces of the cylinders were examined. This was done on the one hand to determine whether the fracture took place within the polyurethane or between the polyurethane and the mortar surface and on the other hand to determine the exact contact area between the polyurethane and the mortar. The zones on the mortar surfaces covered by polyurethane were colored with a black marker (Fig. 3) and the mortar surfaces were scanned. The contact area between polyurethane and mortar was then determined by calculating the number of black pixels on both mortar surfaces in each scan with the program Adobe Photoshop. In this way, the percentage of the mortar surface covered by polyurethane could be determined.

The bond strength of the polyurethanes was calculated by dividing the maximum registered load by the contact area between the polyurethane and the mortar. For the determination of the elasticity of the polyurethanes, the stress-strain curves were calculated. This was done by dividing the registered load by the contact area of polyurethane and dividing the registered elongation by the original length of the polyurethane, which was equal to the simulated crack width of 300 μm. The mean registered strain of the LVDTs at the maximum load (or maximum stress) was then taken as a parameter to evaluate the elasticity of the polyurethanes. However, for most of the specimens one of the three LVDTs registered a shortening of the polyurethane instead of an elongation. This was caused by the fact that the tensile force generated by the testing machine was never perfectly perpendicular to the simulated crack surface. For those specimens the mean strain at maximum load was calculated from two of the three LVDTs that registered an elongation.

Capillary Water Absorption Test

The main aim of self-healing concrete is giving the concrete the ability to heal cracks without human intervention. Healing of the cracks is necessary to prevent the ingress of aggressive substances into the concrete matrix. Water commonly acts as a medium for the transport of these substances, so water ingress is a good parameter to evaluate the healing efficiency. Since capillary absorption dominates water ingress in most concrete structures, water absorption tests were performed on sound, cracked, and healed prismatic mortar specimens.

Seven days after crack creation, all mortar samples were taken out of their respective environments (20 or 50°C) and placed in an oven at 40 ± 2°C until constant mass was achieved in order to obtain an even moisture level. As mentioned previously, constant mass was assumed when a mass change less than 0.1% was obtained in 24 h. When the specimens were dry, the side surfaces were covered over a height of 25 mm with aluminum butyl tape. This ensured that the entrance of water could only occur through the cracked test face. Due to the layer of rubber butyl mass, the tape could be pressed against the mortar surface and a watertight sealing was obtained. A large part of the test face of the samples was also covered with the tape so that there was only a small area of 20×40 mm around the crack exposed to water during the absorption test (Fig. 4).

The absorption tests were carried out based on the European standard NBN EN 13057 (European Committee for Standardization 2002) in an air-conditioned room with a temperature of 20 ± 2°C and a relative humidity of 60%. First, the initial mass of the specimens was recorded. After that, the specimens were placed on two line supports in a shallow tray containing water such that the depth of immersion of the specimens was 2 ± 1 mm. At several time intervals the mass of the specimens was registered using a balance with an accuracy of 0.01 g. Before placing the specimens on the balance, the surplus water at the immersed surface was removed

Fig. 3. Polyurethane on the crack surface: (a) after performance of an axial tensile test; and (b) after the polyurethane was colored with a black marker.

J. Mater. Civ. Eng., 2018, 30(7): 04018145

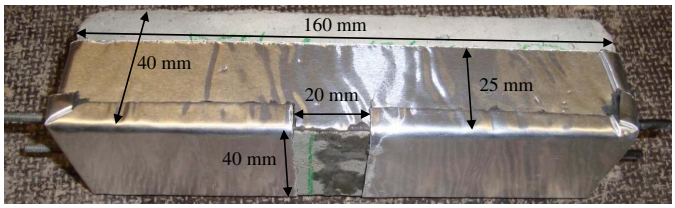

Fig. 4. Mortar sample with a healed crack covered with aluminum butyl tape. Test area of 20 × 40 mm around the crack was exposed to water during the absorption test.

with a wet cloth. After the mass was recorded, the samples were immediately returned to the tray. During the first 8 h of the absorption test, the specimens were weighed every half hour. After that, the specimens were weighed again after 24 and 48 h of water exposure.

One out of three specimens of each series was used to evaluate the healing inside the crack. In order to do so, the hardened polyurethane at the bottom of the specimen was removed by sawing off the outermost 1-mm layer of the bottom of the specimen. After that, the samples were dried again at 40 ± 2°C until constant mass was achieved. Subsequently, the specimens were subjected to a second water absorption test.

Strength Regain

Cracks in cementitious materials do not only impair the durability of the element due to ingress of water and aggressive substances, but also cause a reduction in strength. Therefore, it would be interesting if crack healing would not only be able to seal the cracks but also (partly) cause a recovery of the strength of the material.

The mechanical properties of the prismatic specimens with healed cracks were evaluated by reloading the specimens. For two out of three specimens of each series the aluminum butyl tape was removed and the specimens were reloaded in three-point bending. The peak load of the obtained loading curves was used as an indication for the strength. The strength regain was then calculated by dividing the peak load of the reloading curve by the peak load obtained during the first loading, as stated by Van Tittelboom et al. (2011b).

Visualization of the Crack Healing by X-Ray Computed Tomography

In order to have a better idea about the healing of the specimens inside the crack, five different specimens were scanned using XCT. One specimen of the series of samples healed with polyurethane C at 20 and at 50°C, one specimen of the series of samples healed with polyurethane E at 20 and 50°C, and one specimen with an untreated crack were chosen. The specimens were selected based on the results of the properties of the other experiments. Since only the central part of the specimens where the crack was located was important, the length of the specimens was reduced by sawing off the end parts. The final specimens had a length of 70 mm.

The experiments were performed on a micro-computed tomography (CT) setup called HECTOR at the Centre for X-ray Tomography of Ghent University (UGCT) (Masschaele et al. 2013). The system consisted of a microfocus X-ray source, a flat panel detector measuring 400 mm × 400 mm, and an air-bearing rotation stage. A schematic representation of the sample positioning on the rotation stage is shown in Fig. 5. The specimens were placed in a way that their longitudinal axis coincided with the rotation axis of the stage. In this way, the X-ray beam only needed to pass through a

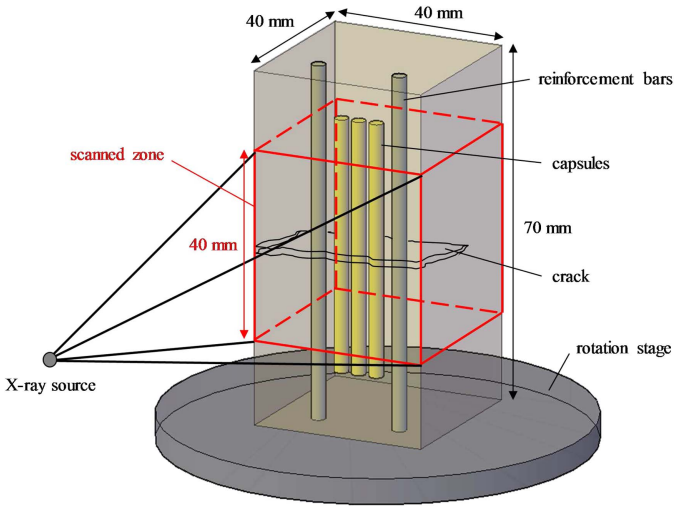

Fig. 5. Position of a sample on the rotation stage in the micro-CT setup. The marked rectangular zone represents the scanned volume.

maximum of 56.6 mm of mortar, which was necessary to obtain a good signal to noise ratio. A central volume of 40 × 40 × 40 mm around the crack was scanned (Fig. 5). The mortar specimens were scanned with a tube voltage of 200 kV and a target power of 35 W. Further, a 0.5-mm-thick copper filter was installed in front of the source to reduce beam hardening and a magnification of 6.14 was obtained. A total of 3,000 projections were taken with a rotation interval of 0.12°. The exposure time of each projection was 1,000 ms. The resulting image size was 1,000 × 1,000 pixels with a pixel size of 0.2 mm. The XCT images were reconstructed into a stack of slices using the Octopus Reconstruction software (Vlassenbroeck et al. 2007), three-dimensional (3D) image analysis was performed with Octopus Analysis (formerly Morpho+) (Brabant et al. 2011), and the volumes were rendered using VGStudio MAX software. The reconstructed voxel size amounted to 32 μm.

Statistical Data Analysis

The obtained results from the different experiments were statistically analyzed with the software program SPSS 23. To compare two mean values, a two-tailed *t*-test was performed with a level of significance of 5%. The comparison of multiple averages was done by using an ANOVA test, also with a level of significance of 5%. The homogeneity of the variances was verified by means of a Levene's test (level of significance of 1%). For data with homogenous variances, a Student-Newman-Keuls (S-N-K) test was performed. If no homogenous variances were obtained, a Dunnett's T3 test was used.

Results and Discussion

Polyurethane Surface Coverage

As mentioned previously, after the performance of the axial tensile tests on the polyurethanes, the fracture surfaces on both cylinder halves were examined. For all of the developed polyurethanes the fracture appeared almost completely between the polyurethane and the mortar surface. This means that the adhesion between mortar and the polyurethane was weaker than the cohesion of the

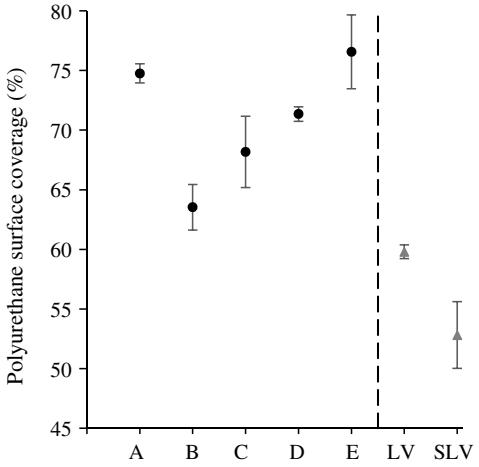

Fig. 6. Mean values of the percentage of mortar surface covered by polyurethane for all newly developed products (descending viscosities from A to E) and commercial products LV and SLV. Error bars represent the standard error of the mean values.

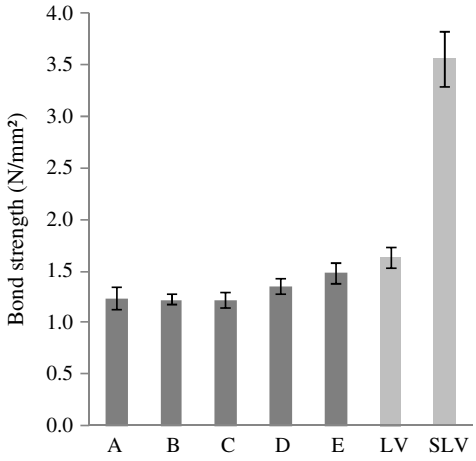

Fig. 7. Bond strength of the polyurethanes. Error bars represent the standard error of the mean values.

polyurethane. The same conclusion could be made for the two one-component commercial healing agents LV and SLV.

The percentage of mortar surface covered by polyurethane for the different healing agents is given in Fig. 6. The mean covered area of all the newly developed products was 10–20% larger than the covered area obtained for the commercial products. After statistical analysis the polyurethane surface coverage of SLV was found to be significantly different from all other polyurethanes. The surface coverage of LV only appeared to be significantly different from Products A, D, and E. Also, the covered area increased when the viscosity of the precursor was lower and the NCO content was higher, with exception of Product A. This was logical since a less viscous precursor will spread more equally over the mortar surface.

By multiplying the percentages of mortar surface covered by polyurethane with the total mortar surface of the cylinders, the exact contact area between the mortar and the polyurethane was calculated. This area was needed to calculate the bond strength and elasticity of the healing agents.

Bond Strength

As was concluded in the previous section, the fracture of the developed polyurethanes occurred almost completely at the interface between the healing agent and the mortar surface. For that reason, the bond strength between the polyurethanes and the mortar is an important parameter regarding the conservation of the healing efficiency of elements subjected to cyclic heating.

The bond strengths of the different polyurethanes are shown in Fig. 7. The mean bond strength of the new polyurethanes used in this research ranged from 1.21 to 1.48 MPa. These bond strengths were comparable to (and not significantly different from) the bond strength of the commercial Product LV (1.63 MPa). The mean bond strength of Product SLV (3.55 MPa) was more than twice the mean bond strength of all other polyurethanes. Consequently, the bond strength of Product SLV was found to be significantly different from the bond strength of all other products.

A trend could also be noticed between the bond strength of the product and the viscosity of the precursor. The bond strength generally increased with decreasing viscosity (and increasing NCO content) of the precursor.

Elasticity

In order to follow movements of cracks due to cyclic thermal loading, the elasticity of the polyurethane is a very important parameter. The mean strain recorded at the maximum load of the polyurethanes was chosen as a parameter to evaluate their elasticity. The higher this value, the more elastic the polyurethane, and consequently the polyurethane will be more able to follow opening and closing of cracks due to cyclic loading. Fig. 8 shows the results of the mean strain at maximum load for all products.

For the newly developed products, the strain at maximum load of the individual specimens varied from 0.5 to 1. The mean strains at maximum load of the commercial products LV and SLV were 0.39 and 0.27, respectively. This shows that the elongation of the newly developed polyurethanes was always higher than what was noticed for the commercial products. However, after statistical analysis, only the strain of Product SLV was found to be significantly different from all newly developed products. For Product E, for example, the mean strain at maximum load was more than three times higher than for Product SLV. This means that the allowable crack movement of the healed crack will also be more than three times higher.

In Fig. 8 a clear increasing trend for the strain at maximum load of the product with decreasing viscosity (and increasing NCO

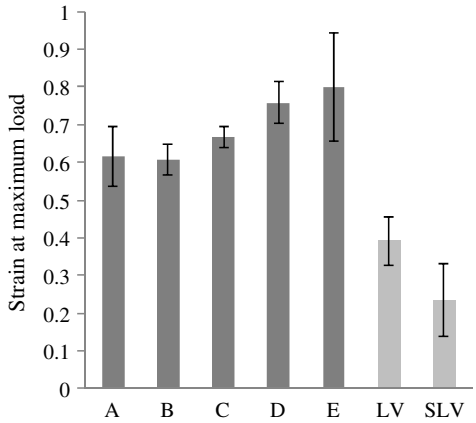

Fig. 8. Strain at maximum load of the polyurethanes. Error bars represent the standard error of the mean values.

J. Mater. Civ. Eng., 2018, 30(7): 04018145

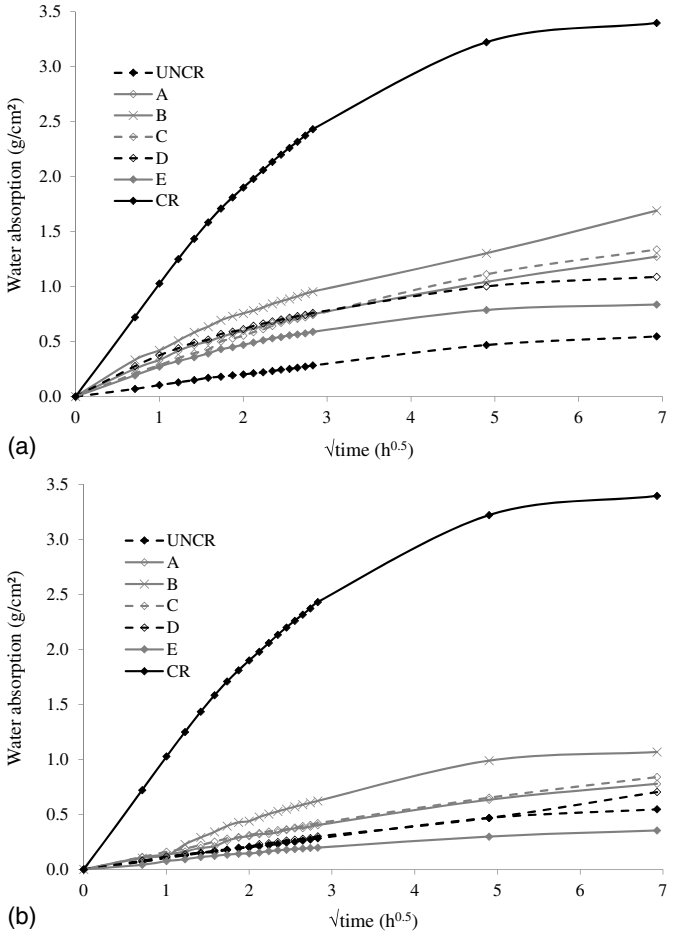

Fig. 9. Cumulative water absorption per unit of surface area exposed to water as a function of the square root of time for specimens stored at (a) 20°C; and (b) 50°C. UNCR and CR reference specimens were stored at 20°C. Error bars were omitted from the graphs in order to keep them clear.

content) of the precursor can be observed. This same increasing trend was also noticed for the bond strength.

Capillary Water Uptake

The total mass of absorbed water during the capillary sorption test was calculated by subtracting the registered mass of the sample at certain time intervals by the initial mass. The value of absorbed water was then divided by the surface area of the mortar exposed to water, which was 800 mm^2 for all specimens. As a result, the cumulative water absorption per unit area (g/cm^2) was plotted in function of the square root of immersion time ($h^{0.5}$) (Fig. 9).

In Fig. 9, the mean absorption curves are plotted for uncracked (UNCR) and cracked (CR) specimens and specimens healed with the different developed polyurethanes (A–E). The error bars were omitted from the graphs in order not to overload them and keep them clear. Fig. 9(a) represents the mean water absorption of the specimens where healing occurred at 20°C, and Fig. 9(b) gives the mean water absorption of the specimens where healing occurred at 50°C. The uncracked and cracked reference specimens were stored at a temperature of 20°C.

Fig. 9(a) shows that the water absorption of the mortar specimens with a healed crack was always in between the water absorption of uncracked and cracked mortar specimens when the healing occurred at a temperature of 20°C. After 24 h, the water absorption of the specimens with a healed crack was 2.5–4 times lower than and significantly different from the water absorption of specimens with an untreated crack. At each time step the self-healing efficiency of the different polyurethanes was evaluated. The efficiency was defined as the ratio of the difference in water absorption between the cracked and the healed sample over the difference in water absorption between the cracked and the uncracked sample. In Table 3, the self-healing efficiency of the polyurethanes for samples healed at 20°C is given. One can see that the self-healing efficiency did not vary much over time (maximum variation of 10% between 1 and 48 h of exposure). This indicated that the healing of the cracks was not only efficient in the initial stage of the water absorption, but stayed effective during the whole immersion period. After an immersion time of 24 h, the self-healing efficiency of all healed specimens stored at 20°C ranged between 70 and 88%. Overall it can be stated that the healing performance of the different products was not significantly different when the healing occurred at a temperature of 20°C. However, the best healing performance at every time step was found for Product E.

Table 3. Self-healing efficiency (%) of the polyurethanes for samples healed at 20°C

Specimen	1 h	2 h	3 h	4 h	5 h	6 h	7 h	8 h	24 h	48 h
A	75	75	76	77	77	77	78	78	79	75
B	66	66	66	67	68	68	68	69	70	60
C	80	81	79	79	79	78	78	79	77	72
D	71	73	75	76	76	77	77	78	81	81
E	82	84	84	84	84	85	85	86	88	90

Table 4. Self-healing efficiency (%) of the polyurethanes for samples healed at 50°C

Specimen	1 h	2 h	3 h	4 h	5 h	6 h	7 h	8 h	24 h	48 h
A	97	97	95	94	94	94	94	94	94	92
B	98	89	86	86	85	84	84	84	81	82
C	94	94	93	93	93	94	94	94	93	90
D	99	100	100	100	99	99	99	99	100	94
E	103	103	103	103	103	103	104	104	106	107

For the specimens where the healing occurred at 50°C [Fig. 9(b)], the water absorption for all products was less than when healing occurred at 20°C. Consequently, a higher self-healing efficiency (Table 4) was found for healing at 50°C compared with healing at 20°C. For Products D and E, the healing efficiency was even 100% or more. This means that the amount of absorbed water in a specimen with a healed crack was even lower than the water absorption of a specimen without a crack. The high self-healing efficiency of these products could be attributed to the fact that the viscosity of these two products at 50°C was very low and consequently a lot of polyurethane leaked out of the capsules into the crack. For some specimens a big part of the mortar surface that was exposed to water during the absorption test was covered with polyurethane. The water absorptions of all healed specimens at 50°C were not significantly different from each other, but they were significantly different from the water absorption of the specimens with an untreated crack (except for Product B due to the very large standard error). Product E again showed the best self-healing efficiency, reaching a value of 106% at 24 h of immersion.

In order to make a clear comparison between the different healing products at different temperatures, the sorption coefficient S ($kg/m^2/h^{0.5}$) of all series was determined. This sorption

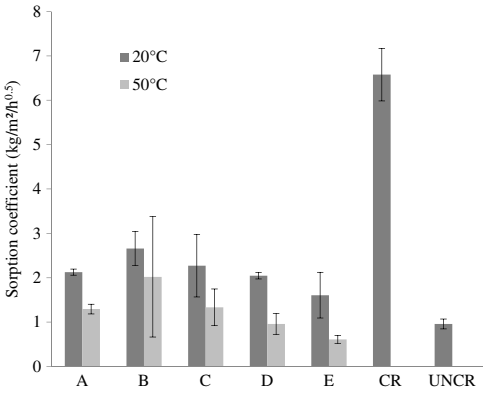

Fig. 10. Capillary sorption coefficients of UNCR, CR, and healed mortar specimens (at 20 and 50°C). Error bars represent the standard error on the mean values.

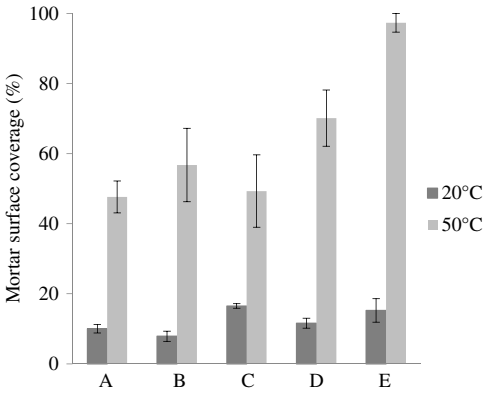

Fig. 11. Percentage of mortar surface (exposed to water during the absorption test) covered by polyurethane. Error bars represent the standard error on the mean values.

coefficient was calculated according to the standard NBN EN 13057 (European Committee for Standardization 2002) as the gradient of the line from the intercept of the water absorption curve to the cumulative mass of the water uptake per unit area recorded at 24 h. In Fig. 10 the sorption coefficients of all specimens are presented.

For crack healing with the new products at both 20 and 50°C, a decreasing trend in the sorption coefficient was noticed when the viscosity of the polyurethane precursor was lower (with the exception of Product A). When the viscosity of the precursor is lower, it can flow out of the capsules more easily after crack creation and thus fills up a larger part of the crack volume. This results in a better healing of the crack and consequently a lower water ingress.

When comparing the products separately at 20 and 50°C, the same conclusions can be drawn as mentioned previously. The sorption coefficient of the specimens healed at 50°C was always lower than when healing occurred at 20°C. For Products D and E, the sorption coefficient of the specimens was reduced by 50% or more when healing occurred at 50°C compared with healing at 20°C. However, after statistical analysis the water absorption for the healed specimens appeared to only be significantly different at 20 and 50°C for Products A and D. This was a result of the high standard errors that were found for the sorption coefficients of healed specimens with Products B, C, and E.

From a durability point of view, the performance of all healing agents for crack healing at high temperatures was satisfactory. The healing of cracks at a temperature of 50°C almost completely prevented water ingress through the crack. This means that aggressive substances will not be able to enter through the cracks anymore, which has a positive effect on the durability and the service life of the construction element. From an esthetic point of view, however, it must be noted that there was still some leakage of polyurethane on the surface of the mortar for all healing products, even for Product A with the highest viscosity. Clearly the viscosity is not the only parameter that determines the amount of healing agent flowing into the crack. Reducing the amount of available healing agent may also lead to a reduction of the polyurethane leakage at the surface. This could be done by reducing the number of capsules in the cementitious matrix or by reducing the length and/or diameter of the capsules. Also, the concrete cover on the capsules could be varied.

Effect of Mortar Surface Coverage by Polyurethane on Capillary Water Uptake

As mentioned previously, some leakage of polyurethane was noticed at the bottom of the specimens. The hardened polyurethane at the bottom covered part of the mortar area exposed to water during the absorption test, especially for the mortar prisms where the crack was healed at 50°C. Therefore, the healing efficiency of the crack itself was evaluated by sawing off the outer layer of the specimens and thus removing the hardened polyurethane at the exposed surface.

The percentage of the mortar zone exposed to water during the absorption test that was covered with polyurethane was determined by means of the program Adobe Photoshop. Fig. 11 shows the results of the mortar zone coverage.

In Fig. 12, the comparison of the sorption coefficients of the specimens before and after removal of the outer layer is shown. In this graph the increase (positive) or decrease (negative) in the sorption coefficient (%) for each specimen of each series is also given. The sorption coefficients of cracked and uncracked mortar specimens are also given in Fig. 12 as a reference.

A first conclusion that can be drawn from Figs. 11 and 12 was that the healing agents that caused a mortar surface coverage of more than 50%, i.e., Products B, D, and E at a temperature of 50°C, showed the highest increase in water absorption after removal of the outer layer (77–122%). This was logical since the polyurethane that hardened at the bottom of the specimens was much less permeable than mortar. Although the water absorption in the

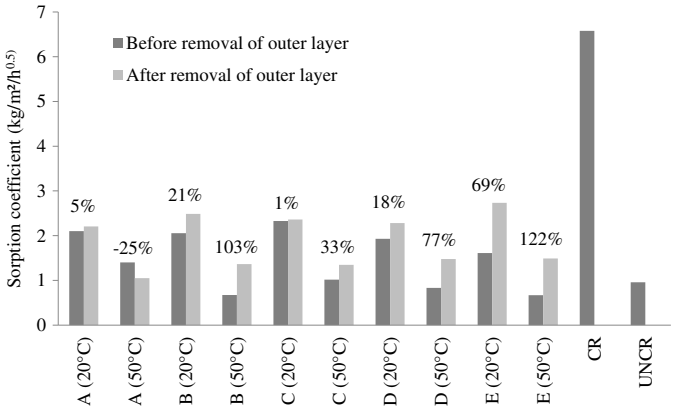

Fig. 12. Capillary sorption coefficients of specimens before and after removal of the outermost bottom layer (one specimen for each series). The increase (positive) or decrease (negative) in sorption coefficient (%) is given above the bars for each specimen of each series.

specimens where the cracks were healed with these products increased a lot when the excess polyurethane at the bottom was removed, the sorption coefficient (and total water absorption) was still less than the sorption coefficient of specimens healed with the same products at 20°C and a lot less than the sorption coefficient of specimens with untreated cracks. The self-healing efficiencies of the mentioned products were still between 91 and 93%. This means that although a lot of polyurethane leaked out of the crack, the polyurethanes were able to fill and consequently heal the inside of the crack. For the specimens where the crack was healed by the other two products at 50°C, less increase (Product C) or even a decrease (Product A) in water absorption was found after removal of the outer layer.

When the specimens were healed at a temperature of 20°C, a relatively small increase in sorption coefficient of 1–21% was found for Products A, B, C, and D (Fig. 12). Since the surface coverage of these products at 20°C was also relatively small (less than 20%), the healing efficiency of these products inside the crack was similar to the healing efficiency at the mouth of the crack (at the mortar surface). For Product E, however, a larger increase of 69% was found. This indicated that the healing efficiency of this product at 20°C inside the crack was not as good as the healing efficiency at the mortar surface.

Finally, it can be concluded that although the water absorption of most specimens increased when the hardened polyurethane at the bottom of the samples was removed, healing of the cracks still caused a large decrease in the total water absorption compared with untreated cracks. The self-healing efficiency of the inner crack for all polyurethanes at both 20 and 50°C still amounted to 60–95%.

Strength Regain

Two specimens of each series were used to evaluate the mechanical properties of the crack healing by reloading. In Fig. 13 the strength regain for the specimens with untreated and healed cracks are shown. For Products A (50°C) and B (50°C), only one specimen could be reloaded due to accidental damage of one of the specimens of these series.

The specimens with untreated cracks show a mean regain in strength of 14%. This strength regain can be attributed to the hysteresis at the beginning of the reloading (Van Tittelboom et al. 2011a; Granger et al. 2007). For crack healing at 20°C, the strength regain varied from 29 to 63% for all products. For Products A–D an increasing trend in strength regain with decreasing viscosity can be seen. This increasing trend was also noticed for the bond strength of the polyurethanes (Fig. 7). An exception to that was Product E, where the regain in strength after autonomous crack healing was low compared with the bond strength of this polyurethane. However, clear conclusions could not be made for this product since the standard error was very large: one specimen showed a strength regain comparable to Product D, while the other specimen showed almost no regain in strength.

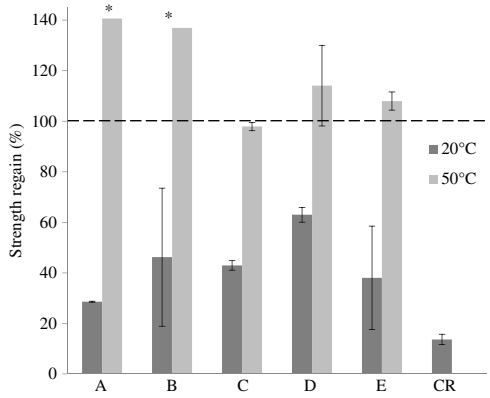

Fig. 13. Regain in strength for untreated cracks (CR) and cracks healed by the different polyurethanes (A–E) at 20 or 50°C. Error bars represent the standard error on the mean values ($n = 2$). The dashed line indicates a value of 100% strength regain. For Series A (50°C) and B (50°C), only one specimen could be reloaded due to accidental damage of one of the specimens.

When crack healing occurred at a temperature of 50°C, the results of the regain in mechanical properties were much better. For all products, a minimum strength regain of 96% was obtained. This means that the polyurethanes were able to restore or even increase the original strength of the material when crack healing occurred at high temperatures. The main reason for this can be attributed to the fact that the viscosity of the polyurethanes was much lower at 50°C, so the polyurethanes were able to flow into the crack more easily and cover a larger part of the crack volume. Also, the hardened polyurethane at the bottom surface of the specimens may have contributed to a part of the large strength regain. No relationship between the regain in strength and the viscosity of the polyurethane precursor was found for healing at 50°C.

Visualization of the Crack Healing by X-Ray Computed Tomography

For one specimen of each series, the hardened polyurethane at the bottom of the specimen was removed and the specimens were subjected to a second water absorption test in order to have a first indication about the healing efficiency of the inner crack. However, it was still uncertain whether the different polyurethanes at different temperatures were able to fill the whole crack space. For this reason, healing of the inner crack was also visualized by X-ray computed tomography.

Visualization was done for four specimens where the cracks were healed with two different healing agents (C and E) at 20 and 50°C as well as a specimen with an untreated crack. Product E was selected because it showed the highest polyurethane surface coverage (Fig. 6), the highest bond strength and strain (Figs. 7 and 8), and the lowest capillary water absorption at both 20 and 50°C (Fig. 9) of all developed polyurethanes. However, healing of a crack with this polyurethane precursor at 50°C had the undesirable effect of leakage of polyurethane at the mortar surface due to the low viscosity of the precursor (Fig. 11). From the developed precursors with similar chemical composition, Product C was selected as the second healing agent used for visualization by XCT. Crack healing with this last product at 50°C showed much less leakage of polyurethane at the mortar surface and it had the highest strain to bond strength ratio.

An analysis of the crack healing was done in VGStudio MAX based on the gray values of the projected data. Air, mortar, and polyurethane attenuate the X-rays in a different way and consequently are represented by a different range of gray values in the projected and reconstructed images. In order to make a clear visualization of the different elements, an artificial color was assigned to the gray value range of each element after simple segmentation.

In order to visualize the crack healing, the resulting 3D data set was reduced to a series of two-dimensional (2D) images by taking cross sections of the 3D render. For each of the healed samples, three cross sections in the length direction of the specimen were visualized. Each cross section ran through one of the three capsules. For

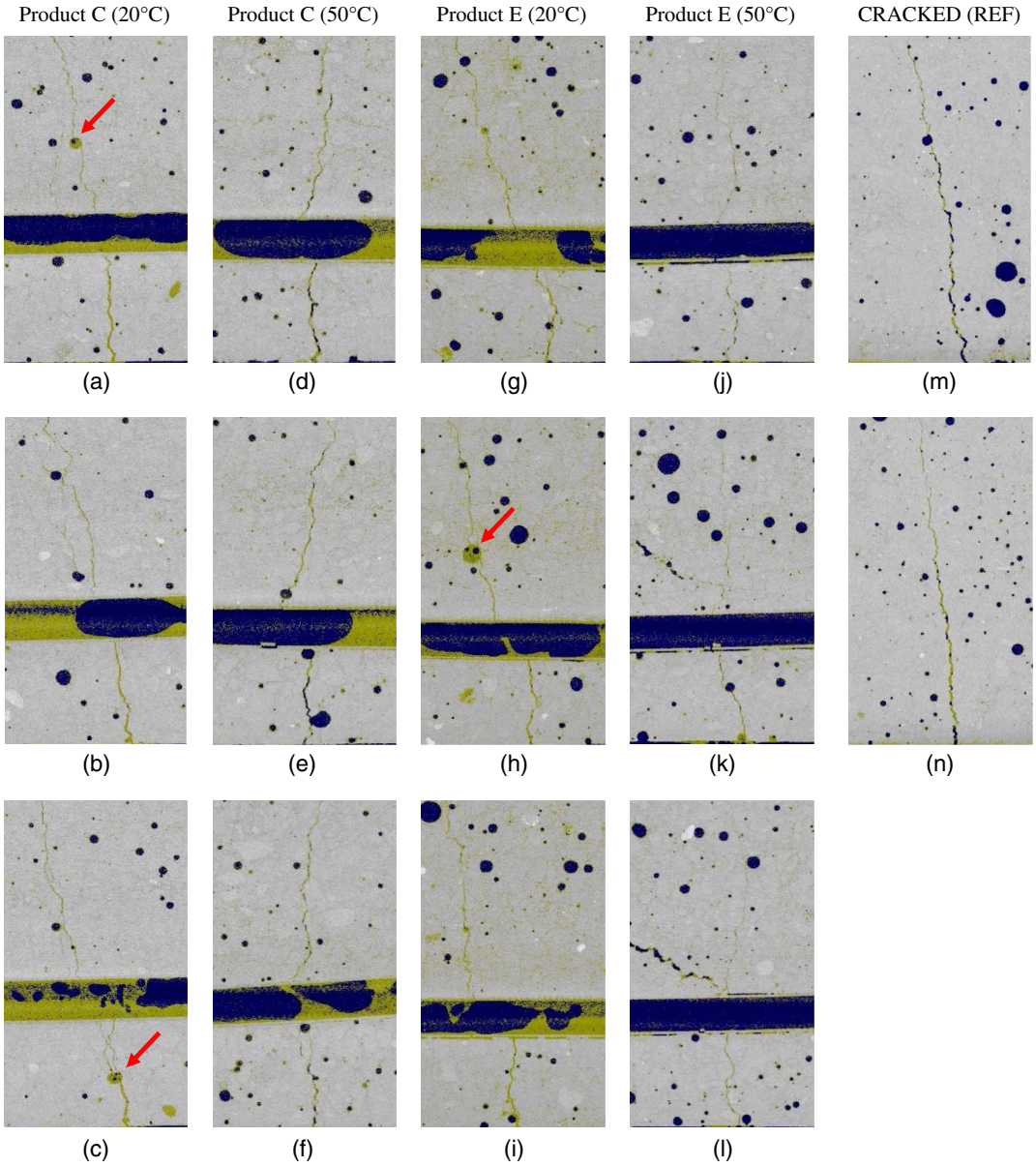

Fig. 14. Visualization of the crack region by XCT cross sections along the length of the specimens for a specimen healed with Product C at (a–c) 20°C and (d–f) 50°C; a specimen healed with Product E at (g–i) 20°C and (j–l) 50°C; and (m and n) a specimen with an untreated crack. The arrows in (a), (c), and (h) indicate pores that crossed the crack path and were filled with polyurethane.

the specimen with an untreated crack, only two cross sections were made. Fig. 14 shows the 2D images of the central region of each section where the crack was located. For the specimens where the crack was healed with Product C at both 20°C [Figs. 14(a–c)] and 50°C [Figs. 14(d–f)] and the specimen healed with Product E at 20°C [Figs. 14(g–i)], the capsules contained some zones with the artificial color assigned to air and some other zones with the artificial color assigned to polyurethane. This indicates that some healing agent remained in the capsules and only part of the healing agent leaked in the crack. Figs. 14(j–l), however, show that for the specimens healed with Product E at 50°C the capsules were completely empty. This was not surprising since for this specimen a lot of leakage of healing agent at the bottom of the specimen was noticed (Fig. 11). The exact amount of healing agent that was still in the capsules could not be determined since only part of the capsules around the crack was visualized by the XCT scan.

In all images of the healed specimens [Figs. 14(a–l)], most of the crack had the artificial color assigned to polyurethane. This could indicate that the cracks were indeed well filled by polyurethane. Also, in Figs. 14(a, c, and h) some pores that were crossing the crack path had the artificial color assigned to polyurethane (indicated by the arrows), indicating that they were filled with polyurethane. This provides a proof that the polyurethane was drawn into the crack by capillary suction and that the part of the crack above the capsules was also (partly) filled with polyurethane. However, when looking at the images of the sample with an untreated crack [Figs. 14(m and n)], a big part of the crack had the artificial color assigned to polyurethane. This cannot be polyurethane, so the color had to be attributed to a transition effect. Due to the very small crack width of the specimens, it was possible that the artificial color inside the crack was a result of the transition in gray value of mortar to the gray value of air inside the crack (also called partial volume

effect). Consequently, no clear conclusion about the filling of the cracks could be made based on the CT images.

Conclusions

Five newly developed polyurethanes with different viscosities were tested in this research for their efficiency in self-healing cementitious materials exposed to high temperatures. When cracks are healed in elements exposed to cyclic heating, it is important that the healing agent fills up the cracks as much as possible and is flexible enough to follow crack movements. By manually applying polyurethanes in simulated cracks, a general increasing trend was found in the polyurethane mortar surface coverage with decreasing viscosity of the polyurethane precursor. Moreover, the surface coverage of the new polyurethanes was found to be 10–20% higher compared with the tested commercial ones. After conducting axial tensile tests, the new polyurethanes also appeared to be much more elastic than the commercial products. The mean strain at maximum load of the new products was found to be 2.6–3.4 times higher than for the commercially available polyurethanes. Consequently, the new polyurethanes will be able to follow much larger crack movements. Moreover, it was found that the elasticity increased with decreasing viscosity of the polyurethane precursor.

After the determination of the mechanical properties of the polyurethanes, the different precursors were encapsulated and the healing action was triggered at two different temperatures (20 and 50°C). The self-healing efficiency was evaluated by capillary sorption tests. At both temperatures the mean sorption coefficient decreased with a decreasing viscosity of the polyurethane precursor (with exception of Product A with the highest viscosity). For four out of five products, the capillary absorption of the samples was reduced by 50% or more when healing occurred at 50°C compared with healing at 20°C. For these products the healing efficiency was as much as 100% or more, meaning that the amount of absorbed water in a specimen with a healed crack was lower than the water absorption of a specimen without a crack. Even when the excess of polyurethane at the bottom of the sample was removed, a healing efficiency of 91–93% was still found for these products. This indicated that the crack was not only well healed at the surface, but also that the inside of the crack was filled with polyurethane.

With regard to regain in mechanical properties, healing at 20°C caused a maximum regain in strength of 73%. When healing occurred at 50°C, however, the minimum strength regain was 96%. This showed that autonomous crack healing with the developed polyurethanes was able to restore the mechanical properties of the material almost completely when healing occurred at high temperatures.

The use of XCT to evaluate the healing of the inside of the crack was not completely successful due to the low crack width of the specimens. Transition effects from the gray value of mortar at the crack edges to the gray value of air in the crack interfered with the gray value of polyurethane. Therefore, no clear conclusions could be drawn about the filling of the inner crack. However, some pores that crossed the crack path were filled with polyurethane, indicating that the healing agent was drawn into the crack. Also, the amount of healing agent that remained inside the capsules after the healing mechanism was triggered could be qualitatively assessed.

The application of the new polyurethanes as encapsulated healing agents in self-healing cementitious materials exposed to high temperatures seems very promising in improving the durability and extending the lifetime of concrete structures. The improved elasticity and flexibility will result in the capability of following larger crack movements, and the self-healing efficiency of most products at 50°C was more than 90%. Generally, the newly developed product with a lower viscosity showed the best results regarding bond strength, water ingress, and strength regain. From an esthetic point of view, further research regarding the development of a healing mechanism that does not show any leakage at the surface is still necessary. This could be done by reducing the number of capsules in the cementitious matrix or by adjusting the length, diameter, or cover depth of the capsules.

Acknowledgments

This research was performed in the framework of the project SHEcon under the program SHE (Engineered Self-Healing materials) and was funded by Strategic Initiative Materials in Flanders (SIM) and Flanders Innovation & Entrepreneurship (VLAIO) formerly known as Agency for Innovation by Science and Technology (IWT). The financial support from these foundations is gratefully acknowledged. Kim Van Tittelboom is a postdoctoral fellow of the Research Foundation-Flanders (FWO) (Project Number 12A3314N) and acknowledges its support.

References

Ahmad, I., and N. Mohammad. 2012. "Structural behavior of precast lightweight concrete sandwich panel under eccentric load: An overview." In *Proc., Int. Conf. on Civil and Environmental Engineering Sustainability.* Johor Bahru, Malaysia: Universiti Tun Hussein Onn Malaysia.

Brabant, L., J. Vlassenbroeck, Y. De Witte, V. Cnudde, M. Boone, J. Dewanckele, and L. Van Hoorebeke. 2011. "Three-dimensional analysis of high-resolution X-ray CT data with Morpho+." *Microsc. Microanal.* 17 (2): 252–263. https://doi.org/10.1017/S1431927610094389.

Cnudde, V., and M. Boone. 2013. "High-resolution X-ray computed tomography in geosciences: A review of the current technology and applications." *Earth Sci. Rev.* 123 (Aug): 1–17. https://doi.org/10.1016/j.earscirev.2013.04.003.

Dry, C. 2001. "Design of self-growing, self-sensing and self-repairing materials for engineering applications." In Vol. 4234 of *Proc., SPIE*, edited by A. R. Wilson and H. Asanuma, 23–29. Bellingham, WA: SPIE.

Dry, C., M. Corsaw, and E. Bayer. 2003. "A comparison of internal self-repair with resin injection in repair of concrete." *J. Adhes. Sci. Technol.* 17 (1): 79–89. https://doi.org/10.1163/15685610360472457.

Dry, C., and W. McMillan. 1996. "Three-part methylmethacrylate adhesive system as an internal delivery system for smart responsive concrete." *Smart Mater. Struct.* 5 (3): 297–300. https://doi.org/10.1088/0964-1726/5/3/007.

European Committee for Standardization. 2002. *Products and systems for the protection and repair of concrete structures—Test methods—Determination of resistance to capillary absorption*. NBN EN 13057. Brussels, Belgium: European Committee for Standardization.

European Committee for Standardization. 2016. *Methods of testing cement—Part 1: Determination of strength*. EN 196-1. Brussels, Belgium: European Committee for Standardization.

Feiteira, J., E. Gruyaert, and N. De Belie. 2014. "Self-healing of dynamic concrete cracks using polymer precursors as encapsulated healing agents." In *Proc., 5th Int. Conf. on Concrete Repair Solutions*, 65–69. Belfast, UK: CRC Press.

Feiteira, J., E. Gruyaert, and N. De Belie. 2016. "Self-healing of moving cracks in concrete by means of encapsulated polymer precursors." *Constr. Build. Mater.* 102 (1): 617–678. https://doi.org/10.1016/j.conbuildmat.2015.10.192.

Granger, S., A. Loukili, G. Pijaudier-Cabot, and G. Chanvillard. 2007. "Experimental characterization of the self-healing of cracks in an ultra high performance cementitious material: Mechanical tests and acoustic

emission analysis." *Cem. Concr. Res.* 37 (4): 519–527. https://doi.org/10.1016/j.cemconres.2006.12.005.

Li, V. C., Y. M. Lim, and Y.-W. Chan. 1998. "Feasibility study of a passive smart self-healing cementitious composite." *Composites Part B* 29 (6): 819–827. https://doi.org/10.1016/S1359-8368(98)00034-1.

Maes, M., K. Van Tittelboom, and N. De Belie. 2014. "Efficiency of self-healing cementitious materials by means of encapsulated polyurethane in chloride containing environments." *Constr. Build. Mater.* 71 (Nov): 528–537. https://doi.org/10.1016/j.conbuildmat.2014.08.053.

Masschaele, B., M. Dierick, D. Van Loo, M. N. Boone, L. Brabant, E. Pauwels, V. Cnudde, and L. Van Hoorebeke. 2013. "HECTOR: A 240 kV micro-CT setup optimized for research." *J. Phys. Conf. Ser.* 463 (1): 012012. https://doi.org/10.1088/1742-6596/463/1/012012.

Mihashi, H., and T. Nishiwaki. 2012. "Development of engineered self-healing and self-repairing concrete: State-of-the-art report." *J. Adv. Concr. Technol.* 10 (5): 170–184. https://doi.org/10.3151/jact.10.170.

Petrie, E. M. 2007. "Adhesive families." In *Handbook of adhesives and sealants*, 343–414. New York: McGraw-Hill.

Salmon, D. C., and A. Einea. 1995. "Partially composite sandwich panel deflections." *J. Struct. Eng.* 121 (4): 778–783. https://doi.org/10.1061/(ASCE)0733-9445(1995)121:4(778).

Van Belleghem, B. 2014. "Ontwikkeling van sandwichpanelen met zelfhelende eigenschappen." Master's thesis, Dept. of Structural Engineering, Ghent Univ., Faculty of Engineering and Architecture.

Van Tittelboom, K., et al. 2016. "Comparison of different approaches for self-healing concrete in a large-scale lab test." *Constr. Build. Mater.* 107 (Mar): 125–137. https://doi.org/10.1016/j.conbuildmat.2015.12.186.

Van Tittelboom, K., K. Adesanya, P. Dubruel, P. Van Puyvelde, and N. De Belie. 2011a. "Methyl methacrylate as healing agent for self-healing cementitious materials." *Smart Mater. Struct.* 20 (12): 125016. https://doi.org/10.1088/0964-1726/20/12/125016.

Van Tittelboom, K., N. De Belie, D. Van Loo, and P. Jacobs. 2011b. "Self-healing efficiency of cementitious materials containing tubular capsules filled with healing agent." *Cem. Concr. Comp.* 33 (4): 497–505. https://doi.org/10.1016/j.cemconcomp.2011.01.004.

Van Tittelboom, K., E. Gruyaert, P. De Backer, W. Moerman, and N. De Belie. 2015. "Self-repair of thermal cracks in concrete sandwich panels." *Struct. Concr.* 16 (2): 273–288. https://doi.org/10.1002/suco.201400055.

Van Tittelboom, K., D. Van Loo, N. De Belie, and P. Jacobs. 2010. "Evaluation of the efficiency of self-healing in concrete by means of μ-CT." In *Advances in computed tomography for geomaterials*, edited by K. Alshibli and A. Reed, 133–139. London, UK: Wiley.

Vlassenbroeck, J., M. Dierick, B. Masschaele, V. Cnudde, L. Van Hoorebeke, and P. Jacobs. 2007. "Software tools for quantification of X-ray microtomography at the UGCT." *Nucl. Instrum. Meth. A* 580 (1): 442–445. https://doi.org/10.1016/j.nima.2007.05.073.

Wang, J., J. Dewanckele, V. Cnudde, S. Van Vlierberghe, W. Verstraete, and N. De Belie. 2014. "X-ray computed tomography proof of bacterial-based self-healing in concrete." *Cem. Concr. Comp.* 53 (Oct): 289–304. https://doi.org/10.1016/j.cemconcomp.2014.07.014.